

Article

Preparation and Impact Resistance Properties of Hybrid Silicone-Ceramics Composites

Katarzyna Kośla *, Paweł Kubiak , Marzena Fejdys, Karolina Olszewska, Marcin Landwijt and Edyta Chmal-Fudali

Institute of Security Technologies “MORATEX”, Marii Skłodowskiej-Curie 3 Street, 90-505 Lodz, Poland; pkubiak@moratex.eu (P.K.); mfejdys@moratex.eu (M.F.); itb@moratex.eu (K.O.); mlandwijt@moratex.eu (M.L.); efudali@moratex.eu (E.C.-F.)

* Correspondence: kkosla@moratex.eu; Tel.: +48-42-637-37-10

Received: 25 November 2020; Accepted: 16 December 2020; Published: 19 December 2020



Featured Application: The developed hybrid silicone-ceramic composite can be used as a ballistic inserts in bulletproof vests, which was confirmed by the conducted research. Obtained results indicates that the developed hybrid silicone-ceramic composites are characterized by higher values of the V50 parameter for the FSP.22 fragment compared to the currently used, traditional, ballistic hard plates with a comparable surface mass.

Abstract: This article presents the method of preparation a new type of ballistic armor based on hybrid silicone-ceramic (HSC) composites with considerable flexibility. An experimental study on the ballistic behavior of HSC composites connected with soft body armor is presented against FSP.22 fragments. The effect of Al₂O₃ ceramics on the ballistic performance of HSC composite was investigated, and the fragmentation resistance process of the composite armor combining the HSC composite and soft aramid insert is clarified. Furthermore, impact resistance tests made with a drop tower which allows for a gravity drop of a mass along vertical guides onto a sample placed with an energy of 5 J were performed. The results presented in this paper show that the HSC composites can be successfully used as a hard body armor. However, they do not exhibit the properties of absorbing the impact energy generated during the drop tower tests. The test results show that the ballistic performance of composite armors is influenced by the hardness and Young modulus of ceramics and soft body armor panel. Additionally, in the article, the results of mechanical properties of silicones used for preparation of composites were presented and compiled to determine their role in the performance of impact protection.

Keywords: ballistic protection; impact absorption; body armor; hybrid silicone-ceramic composites; ballistic inserts

1. Introduction

The development of personal protection systems with improved ballistic performance and reduced weight has received a great interest in the last decade with the unfortunate ever-increasing threats and conflicts. Nowadays, ballistic protection systems are being increased in their functionality and technological aspects. Many efforts have been taken to improve their ballistic resistance alongside the weight reduction. Armor systems development works concern many sectors of the economy, including defense and security, where the key role is played by personal protective equipment (e.g., bulletproof vests, ballistic inserts, etc.). Their main objective is to provide adequate impact (ballistic) protection for the user who is exposed to the hazards of loss of life or health due to the nature of his or her work. While applying different ballistic and high performance materials, like ceramic tiles composites and

Twaron/Kevlar based composites, integrated into one armor (ballistic) system, it is also possible to use the personal ballistic protection system, or enforcement for different valuable goods or properties like vehicles, airplanes or military equipment.

Among the systems intended for the implementation of personal protective equipment, such as ballistic vests, body armor plays a leading role. Ballistic body armor is broadly classified into two categories, namely hard body armor and soft body armor. Soft armor should protect the wearer against most common and low to medium energy projectiles which could go up to a velocity of 500 m/s. These types of body armor are mostly made from high performance fibers, such as aramid or Ultra High Molecular Weight Polyethylene (UHMWPE) fibers and are widely used in personnel ballistic protective clothing for military and law enforcement application thanks to typical flexibility and light weight [1–4]. On the other hand, hard body armor was designed to resist projectile velocity of NIJ Standard level IIIA [5], or more than 500 m/s velocity when worn in conjunction with soft armor. Hard body armor is made mainly of metal, composite, or ceramic plates [6–8]. Ceramic materials such as aluminum oxide (Al_2O_3), silicon carbide (SiC), or boron carbide (B_4C) have been widely applied in armor design due to their high compressive strength, high hardness, and low density. High hardness and high compressive strength of ceramic materials contribute to projectile destruction and/or spreading of the impact load on a larger area of the armor during ballistic impact [9–12].

The shape and dimensions of the ceramic elements have a significant influence on the ballistic resistance of the hard body armor. According to Su and Chen's studies [13], the ballistic simulation tests show differences between regular hexagonal and square shapes of ceramic panels. During the research, it was shown that the hexagon units have better performance in the intersection points of panels while the ballistic performance of square unit and regular hexagonal unit is basically the same in central and eccentric areas of panels. Moreover, the results of the simulation were confirmed to the real ballistic test. The ballistic efficiency of alumina tiles with various sizes, shapes, and target configurations was also measured by Song et al. [14]. The ballistic efficiency of square tiles roughly 8 mm thick struck by 12.7 mm diameter bullets rapidly increased with tile size up to about 100 mm. Circular shape tiles had lower ballistic efficiencies than those of square shape tiles for the same width and thickness. The authors explained the obtained results by the effect of reflected waves at edges and the propagation of resulting cracks on the projectile penetration process. In turn, Hazell and co-workers [15] performed tests with different areal geometries silicon carbide square tiles. The tiles were manufactured via two different processes, and have been bonded to polycarbonate layers to evaluate their ballistic performance. Four ceramic tile sizes were tested: 85 mm, 60 mm, 50 mm, and 33 mm, and obtained results showed that there is a crucial dimension of tile that should be used in a silicon carbide-based ceramic-faced mosaic armor system design to ensure its optimum performance. Another comparison of the ballistic performance was made over a series of additively manufactured alumina tiles placed over the back plate, which were investigated using both forward- and reverse-ballistic experiments. The results show some major differences between various types of tiles, increasing its ballistic performance along with the thickness [16].

In general, ceramic hard body armor systems consist of a hard brittle ceramic facing the projectile and a soft deformable backing material. The ceramic destroys the projectile tip, slows it down, and distributes the load over a large area of the backing. The backing supports the ceramics and brings the comminuted ceramics and the projectile to rest. The backing material is selected in structural, ballistic, and weight terms [15,17]. Body armor still has a lot of problems related to weight, ergonomics (especially adjustment to the user's body and air permeability), scope, and area of protection and better energy absorption. For this reason, new solutions in the field of construction and materials are constantly sought to eliminate the above-mentioned disadvantages. In recent years, many solutions have been proved to be very efficient in providing superior ballistic performances and weight reduction [18–23].

Among different hybrid composites, ceramic-polymer composite armors are particularly interesting for their high strength and light weight with high energy absorption capability. While the function of ceramics is to retard ballistic impact penetration, a polymer panel is to absorb high energy

generation from the propagation of elastic/stress waves [24]. Colombo et al. [25] presented studies of composite layered systems based on monolithic armor ceramic tiles joined with polymer infiltrated ceramic foams which have been designed and evaluated for lightweight ballistic protection. Open cell silicon carbide foams of various cell sizes infiltrated with thermosetting or elastomeric polyurethane were used for this design.

In addition, the state of the art research carried out in the field of flexible ballistic shields manufactured based on ceramic and/or elastomeric elements made it possible to indicate a patent application describing a method of making a product in the form of a composite ballistic plate absorbing and dissipating kinetic energy after impact with a high velocity projectile, intended for covers for vehicles or fixed objects. The plate comprises a layer made of individual ceramics pellets or a sintered refractory material. The pellets form regular rows and columns and are bound and held in the form of a plate by the solidified elastic material. A thermoplastic polymer such as polycarbonate or a thermosetting material such as epoxy resin is used as the bonding material. Moreover, the plate may contain layers of woven or non-woven textile material. However, due to its significant surface weight, thickness, and stiffness, this solution is not suitable for use in personal protective clothing [26].

Furthermore, based on the patent description No. PL 224825 [27], the possibility of producing a flexible armor intended for use mainly as an insert for bullet-proof and fragment-proof vests is specified. The armor consists of layers of ballistic textile material between which there is a layer composed of closed pouches, partially overlapping each other. The pouches are filled with STF (Shear Thickening Fluid) or MRF (Magneto Rheological Fluid). The armor provides resistance to penetration by 5.56–14.5 mm small and medium caliber armor-piercing shells and to penetration by fragments or an explosion.

Gamache et al. [28] developed a body armor composite material which include a flexible liner, a polymer binder disposed on the liner, and ceramic solids embedded in the binder. The flexible liner conforms to a portion of the wearer and elastically deforms in response to application of mechanical force. The binder can be a polyurea foam. The solids can be spheres arranged in a single-layer pattern, substantially parallel to liner. Martin and co-workers [29] presented a similar solution—composite material system of armor comprises a strike stratum and a backing stratum. The strike stratum includes elastomeric matrix material and inventive ceramic-inclusive elements embedded therein and arranged (e.g., in one or more rows and one or more columns) along a geometric plane corresponding to the front (initial strike) surface of the strike stratum. More rigid than the strike stratum, the backing stratum is constituted by, e.g., metallic (metal or metal alloy) material or fiber-reinforced polymeric matrix material. Some inventive embodiments also comprise a spall-containment stratum fronting the strike stratum.

Despite the presence of several patent applications and publications, where solutions based on ceramic-polymer composites were discussed, the results of tests of resistance to fragments and impact energy absorption made with a drop tower by silicone-ceramic composites have not been presented so far. The results presented in this paper show that the hybrid silicone-ceramic composites can be successfully used as ballistic hard body armor. However, they do not exhibit the properties related to absorption of the impact energy generated during the drop tower tests. The test results show that the ballistic performance of composite armors is influenced by hardness and Young modulus of Al_2O_3 ceramics and the soft body armor panel. The obtained HSC composites were aimed at improving ergonomic properties by having increased flexibility compared to standard hard body armor made of metal or pressed aramids or UHMWPE sheets.

This work is part of a project aimed at developing a next generation anti-blast and fragment-proof protective suit, designed to provide the personal protection to bomb-disposal experts during their direct operations linked to the explosive devices neutralization. For this reason, the HSC composite was developed for its use in explosion-proof and fragment-proof clothing, which should meet requirements of NIJ Standard 0117.01 [30]. The results obtained may be a reference point enabling the assessment of

the use of hybrid silicone-ceramics composites in armor, personal protective system, and applications related to the ballistic protection of vehicles and other objects.

2. Materials and Methods

2.1. Materials

2.1.1. Silicone Materials

Three types of silicone elastomers were used to produce the hybrid silicone-ceramic composites: Za 22 Mould (Zhermack, Badia Polesine, Italy), MM 228 silicone (ACC Silicones, Bridgwater, England), MM 922 silicone (ACC Silicones, Bridgwater, England). The properties of applied silicone materials are presented in Table 1. Density, hardness, and tear strength under static stretching parameters have been determined in accordance with the test methodology described in points Sections 2.3.1–2.3.3.

Table 1. Technical specification of silicone elastomers applied for the hybrid silicone-ceramic composites.

No.	Parameter	Unit	Results			Test Method
1.	Silicone name	—	Za 22 Mould	MM 228	MM 922	manufacturer's technical specification
2.	Density	g/cm ³	1.09 ± 0.04	1.11 ± 0.01	1.23 ± 0.01	PBCH-09/2017 [31]
3.	Hardness	ShA	20 ± 1	28 ± 2	22 ± 1	PN-EN ISO 868:2005 [32]
4.	Tear strength under static stretching	MPa	3.35 ± 0.16	1.54 ± 0.32	3.64 ± 0.18	PN-ISO-37:2007 [33]
5.	Breaking strength	MPa	4.0	5.06	3.6	
6.	Elongation at break	%	380	746	497	
7.	Tensile strength	kN/m	20.0	31.0	26.2	manufacturer's technical specification
8.	Viscosity	mPas	4000	13,000	19,000	
9.	Lifetime	min	15	55	45–120	
10.	Demolding time	h	1	5	8–12	

2.1.2. Ceramic Materials

To produce the hybrid silicone-ceramic composites, hexagonal ceramics made from aluminum oxide (Al₂O₃ content 98%, CeramTec, Plochingen, Germany) were used. Hexagonal ceramic elements had the following dimensions: side of the hexagon—(11.5 ± 0.2) mm, longer diagonal of the ceramic tile—(23.0 ± 0.2) mm, shorter diagonal of the ceramic tile—(19.9 ± 0.2) mm. The technical parameters of ceramic materials are presented in Table 2. Parameters have been determined in accordance with the test methodology described in Section 2.3.5.

Table 2. Physical and mechanical parameters of Al₂O₃ ceramics (CeramTec, Plochingen, Germany).

Parameter	Density [g/cm ³]	Young's Modulus [GPa]	Acoustic Impedance [10 ⁵ g/cm ² s]	Vickers Hardness [GPa]	Resistance to Brittle Fracturing, [MPa m ^{1/2}]
Test method	PN-EN 993-1:1998 [34]	ASTM C 1419-99a [35]		PN-EN-ISO 6507-1:2007 [36]	
Al ₂ O ₃ 3.0 mm thickness	3.81 ± 0.1	464.0 ± 8.0	40.0 ± 0.2	15.4 ± 0.4	4.29 ± 0.4
Al ₂ O ₃ 3.5 mm thickness	3.81 ± 0.1	472.6 ± 10.0	40.0 ± 0.2	18.9 ± 0.3	4.32 ± 0.3

2.1.3. Additional Materials

The following materials were used as additional reinforcement layers: Poron[®]XRDMA (Polting Foam Sp. zo.o, Gliwice, Poland) and Twaron[®]CT612 (Teijin, Wuppertal, Germany) with the physico-mechanical properties given in Tables 3 and 4. In addition, there were ceramic elements placed on a carrier film which was a self-adhesive film 4622/WS 40 (Bochemia, Radom, Poland) in order to stabilize them and improve the efficiency of the production process of silicone-ceramic composites.

Table 3. Physical and mechanical parameters of the aramid fabric Twaron[®]CT 612 (Teijin, Wuppertal, Germany).

No.	Parameter	Unit	Results of Metrological Tests	Test Method
1	Width	m	1.31 ± 0.01	PN-EN 1773:2003 [37]
2	Areal density	g/m ²	123 ± 1	PN-ISO 3801:1993 [38]
3	Number of threads	-warp -weft cm/dm	112 ± 2 108 ± 2	PN-EN 1049-2:2000 [39]
4	Thickness	mm	0.18 ± 0.02	PN-EN ISO 5084:1999 [40]
5	Maximum force	-warp -weft N	5700 ± 205 5800 ± 211	PN-EN ISO 13934-1:2013-07 [41]
6	Elongation at rupture	-warp -weft %	4.2 5.0	PN-EN ISO 13934-1:2013-07 [41]

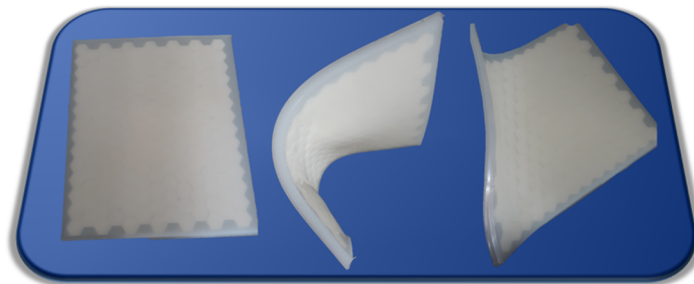
Table 4. Physical and mechanical parameters of the Poron[®]XRDMA (Polting Foam Sp. zo.o, Gliwice, Poland).

No.	Parameter	Unit	Results of Metrological Tests	Test Method
1	Density	g/cm ³	0.19 ± 0.01	PBCH-09/2017 [31]
2.	Thickness	mm	3.0 ± 0.2	PN-EN ISO 5084:1999 [40]
3.	Areal density	g/m ²	555 ± 12	PN-EN ISO 2286-2:2016 [42]
4.	Tensile strength	kPa	446 ± 29	PN-EN ISO 1798:2001 [43]
5.	Tear strength	N/m	297 ± 44	PN-EN ISO 8067:2009 [44]

2.1.4. The Tested System in a Form of a Hybride Silicone–Ceramic Composite and Soft Ballistic Inserts

Hybrid silicone-ceramic composites (HSC) (Figure 1) consist of 5 layers, including:

- outer layers made of elastomer;
- inner layer made of ceramic elements placed on the carrier film;
- reinforcement layers made of aramid fabrics and/or foamed polymer materials.

**Figure 1.** Hybrid silicone-ceramic composite—general view.

The scheme showing the structure of the composite is presented in Figure 2.

In the research conducted, the outer layer consisted of the following silicone elastomers: Za 22 Mold (Zhermack, Badia Polesine, Italy), MM 228 silicone (ACC Silicones, Bridgwater, England) and MM 922 silicone (ACC Silicones, Bridgwater, England). The inner layer consisted of hexagonal ceramic elements based on Al₂O₃ ceramics with a thickness of (3.0 ± 0.2) mm and (3.5 ± 0.2) mm. These elements were placed on a carrier which was a self-adhesive film 4622/WS 40 in order to stabilize them and improve the efficiency of the production process. The following materials were used as reinforcing layers: Poron[®]XRDMA (Polting Foam Sp. zo.o, Gliwice, Poland) and Twaron[®]CT 612 (Teijin, Wuppertal, Germany).

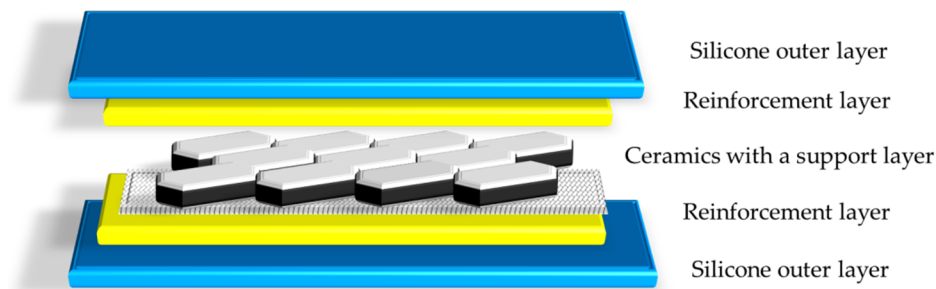


Figure 2. Diagram of the construction of a hybrid silicone-ceramic composite.

Soft ballistic inserts were obtained from combining the sheets of Twaron[®]CT 612 (Teijin, Wuppertal, Germany), with a total areal density of $(5 \pm 0.5) \text{ kg/m}^2$.

2.2. Manufacture of Hybrid Silicone-Ceramic Composites

The outer layers in the form of the Za 22 Mold silicone elastomer were obtained by mixing silicone components A and B (A-base, B-catalyst) in a 1: 1 weight ratio. The MM 228 silicone layer was prepared by mixing the base and standard catalyst in a 10:1 weight ratio. The MM 922 silicone was prepared by mixing the silicone base and the catalyst in a 100:5 weight ratio. The amount of silicone mass to produce a single outer layer containing the base with the catalyst was approximately 300 g.

After the components of the silicone elastomer were mixed in the weight ratio given above, the silicone mass was poured into a mold. So that the silicone pre-cross-links and the remaining layers after their application on its surface do not fall to the bottom of the mold, the mass was left for the period:

- up to 120 min in the case of MM 922 silicone,
- up to 30 min for Za 22 Mold silicone,
- up to 50 min for MM 228 silicone.

Then, a single reinforcing layer—Poron[®]XRDMA with a thickness of $(3.0 \pm 0.2) \text{ mm}$ —was applied to the surface of the silicone layer. Hexagonal ceramic tiles previously stacked on the carrier film were placed on the reinforcing layer. Then another reinforcing layer in the form of a Twaron[®]CT612 sheet was applied. The whole was poured with silicone elastomer and allowed to cross-link. The demolding time of the composite was the minimum: 12 h for MM 922 silicone, 5 h for MM 228 silicone, and 1 h for Za 22 Mold silicone.

2.3. Methods

2.3.1. Density

The basic physical and mechanical parameters of silicone elastomers such as: density, hardness, and tear strength with static tensile were tested according to the methodology described below.

The density of elastomers was determined by the hydrostatic method on the basis of PBCH-09/2017 test procedure “Determination of density by the hydrostatic method”, 2nd edition of 01/12/2017 [31]. The density was calculated from the following formula:

$$\rho = (A/A - B) \times \rho_0 \quad (1)$$

ρ —sample density (g/cm^3),

A—weight of sample in air (g),

B—weight of sample in liquid (g),

ρ_0 —density of liquid (g/cm^3).

2.3.2. Tear Strength with Static Tensile of Silicones

Determination of mechanical properties of silicone elastomers at static tension was performed in accordance with PN-ISO-37:2007 [33]. The tensile test was carried out on standard paddle or ring shaped samples in a testing machine (Instron) at a constant tensile speed. The tensile stress was calculated as the force related to the unit of area of the initial cross-sectional area of the measuring section of the tested elastomer sample. Tensile strength is defined as the maximum recorded tensile stress and elongation at break is defined as the deformation of the measuring section at break. In such a method of determining the tensile strength of elastomers, the effect of transverse deformation of the sample during the test is not taken into account.

2.3.3. Silicone Elastomers Hardness

Silicone elastomers were characterized in terms of their hardness. Hardness measurements were carried out in accordance with PN-EN ISO 868:2005 standard “Plastics and Ebonite—Determination of Identification Hardness by Means of Durometer (Shore Hardness)” [32] using a Shore A hardness tester mounted on a tripod. The hardness result was read after 15 s. Five hardness measurements were made for each sample and the average of the five measurements was given as the result.

2.3.4. Structural Testing of Elastomers Using FT-IR

The research was performed in accordance with the research procedure PBCH-02/2014 “Spectrophotometric analysis of spectra in the aspect of determining the raw material composition in selected textile materials”, 2nd edition of 01/12/2017 [45] using the FTIR-Nicolet iS10 single beam spectrophotometer—THERMO Scientific. In order to perform a correct IR analysis, two measurements were taken: the crystal background spectrum and the sample being tested spectrum. The FTIR spectrum was determined as the ratio of the sample spectrum to the background spectrum (when performing the background spectrum, the response of the spectrometer itself is measured, without the sample). The division of the sample spectrum by the background spectrum (so-called “Rationing”) removes the adverse effects caused by the instrument and weather conditions, so that the signals present in the final spectrum only come from the sample. The measurements were carried out with the use of DTGS KBr detector, with resolution equal to 4.

2.3.5. Methodology of Physical and Mechanical Testing of Al₂O₃ Ceramic Elements

Tests of physico-mechanical properties were conducted for the ceramic materials. Apparent density (ρ), Young’s modulus (E), acoustic impedance (Z), Vickers hardness (HV20), and resistance to brittle fracturing (K_{Ic}) were determined. Apparent density of ceramic was determined by the hydrostatic method according to BS EN 993-1:1995 [34], and resistance to brittle fracturing and Vickers hardness were determined based on the PBS 1-4 procedure according to references [36,46] under a load of 9.8 N. In turn, the velocity of sound propagation, Young’s modulus, and acoustic impedance were determined based on the measurement of the time of a passage of an ultrasound wave through the material tested according to the PBS 5-1 procedure developed under the standards [35]. Tests of physico-mechanical properties of the ceramic materials were conducted at the Department of Ceramics and Refractories, AGH University of Science and Technology, Poland.

2.3.6. Determination of the HSC Composite Mass Per Unit Area

The test was carried out in accordance with PN-EN ISO 4674-1:2017-02 [47], using an analytical balance allowing for weighing with an accuracy of 0.001 g. The mass per unit area was calculated according to the formula:

$$m_p = (m_i/d \times s) \times 10^6 \quad (2)$$

where:

m_i —material mass, [g];

d —material length calculated as an arithmetic mean of 3 length measurements, [mm];

s —material width calculated as an arithmetic mean of 3 width measurements, [mm].

2.3.7. Fragmentation Resistance Test

Samples intended for the assessment of fragmentation resistance were hybrid silicone ceramic composites (HSC) combined with “soft” ballistic inserts sewn into the cover and with mass per unit area of $(5.0 \pm 0.5) \text{ kg/m}^2$. Soft ballistic inserts were created by cutting out and assembling layers of Twaron[®]CT612 para-aramid ballistic material. The inserts were then sewn on the corners. The distance between seams (stitches) was $(1.0 \pm 0.1) \text{ cm}$. The distance from the stitch to the edge was $(2.0 \pm 0.1) \text{ cm}$. The stitches were fixed at the ends with a return stitching (about 1 cm). The PBB-09 2nd edition of 12.2013 Test Procedure [48] based on the requirements and testing methodology contained in Stanag 2920 [49] has been used to determine the fragmentation resistance. For HSC fragmentation, resistance tests combined with soft ballistic inserts, a standard FSP.22 fragment of mass of $(1.10 \pm 0.03) \text{ g}$, diameter $(5.46 \pm 0.05) \text{ mm}$ and length of 6.35 mm, made of steel with hardness of $(27 \pm 3) \text{ HRC}$ was used. The test of fragmentation resistance was conducted in a “dry” state. The sample dimensions were $250 \times 300 \text{ mm}$. The test was conducted at room temperature $(20 \pm 5) \text{ }^\circ\text{C}$ at relative air humidity $(65 \pm 10)\%$. At least six shots were fired to each sample: three causing partial puncture and three causing total puncture. The limit of ballistic protection V50 was determined as an average of the equal number of the highest measured speeds of the fragment causing only partial puncture and the lowest measured speeds causing total puncture within the velocity spread $\Delta \leq 40 \text{ m/s}$.

2.3.8. Impact Tests

Impact tests were performed according to test procedure PBB-07 ed. II: 12.2008 “Impact tests. Determining the level of impact energy attenuation for body protectors” [50], developed based on BS 7971-1:2002 “Protective clothing and equipment for use in violent situations and in training. General requirements” [51], in an accredited Ballistic Testing Laboratory ITB, “MORATEX”. The tests were conducted for hybrid silicone ceramic composites and silicone elastomers using a flat impactor and R 150 cylindrical die. For the impact tests, a Drop Tower was used to drop the mass (“gravitational drop”) along vertical guides with energy $(5 \pm 1) \text{ J}$ on the sample placed on the test die. The principle of operation of the device is as follows: on a sample placed on a die attached to the base, an impactor of a certain mass and energy drops along the vertical guides. During the test, the force transferred to the die under the tested guard is recorded using a piezoelectric force sensor mounted in the die base.

During the above mentioned tests, a drop impactor of weight $(5000 \pm 10) \text{ g}$, made of polished steel with a flat surface of $40 \times 80 \text{ mm}$ and rounded edges $(50 \pm 5) \text{ mm}$. A semi-circular die with a 50 mm radius and height of $(180 \pm 20) \text{ mm}$, made of polished steel, was also used. The tests were carried out under ambient conditions, but previously the samples were acclimatized for $(48.0 \pm 0.5) \text{ h}$ at $(23 \pm 2) \text{ }^\circ\text{C}$ and relative humidity $(50 \pm 5)\%$. The tests were performed for hybrid silicon-ceramic composites, samples obtained from silicones previously used to produce HSC and material samples obtained from polymers used commercially as impact energy absorbers.

3. Results and Discussion

3.1. Analysis of the Results of Physical, Mechanical and Structural Tests of Silicones Used for the HSC Composites Production

In the first phase of the work, the physico-mechanical parameters of silicones used to produce HSC composites were determined and their chemical structure was compared by performing and analyzing infrared spectroscopy spectrums. Physical-mechanical parameters of silicones used to prepare composites are presented in Table 1.

The lowest values of parameters, i.e., hardness, elongation at tear, tensile strength, density, and viscosity, are provided by Za 22 Mould silicone (Zhermack, Badia Polesine, Italy). This silicone is also characterized by the shortest lifetime and demolding time, which is an important element in semi-technical and industrial processing. The highest parameters of hardness, tear strength, elongation at tear, and tensile strength are characterized by MM 228 silicone (ACC Silicones, Bridgwater, England). Later on, FT-IR structural tests of silicones used to produce hybrid silicon-ceramic composites were also conducted. The obtained FT-IR spectrums are shown in Figure 3.

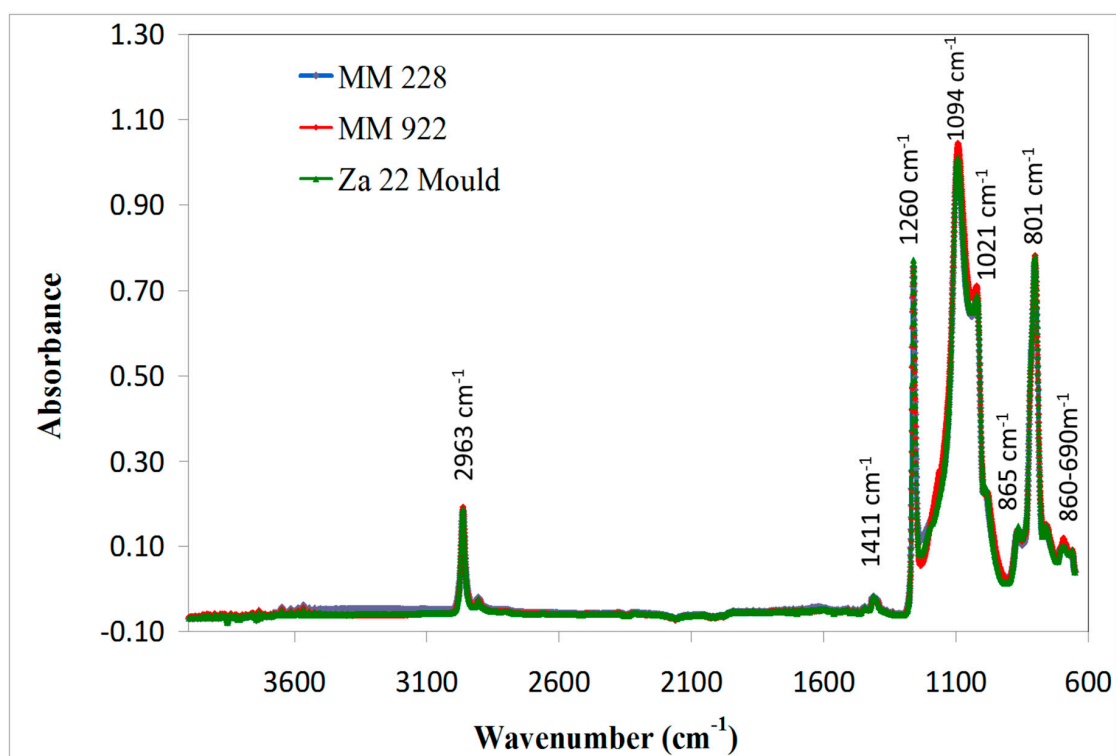


Figure 3. FT-IR spectra of silicone elastomers used to make hybrid silicone-ceramic composites.

The spectrums obtained for each of the three silicones used to obtain hybrid silicon-ceramic composites are characterized by the occurrence of bands at wavenumbers of 660–690 cm^{-1} , corresponding to bending oscillation of single carbon bonds. The presence of a low intensity band in the wavenumber range 761 cm^{-1} corresponding to bending vibrations of C–H bonds was also observed. Moreover, the presence of bands at wavenumbers of 801 cm^{-1} and 865 cm^{-1} was observed from deformed pendulous oscillation of $\text{CH}_3\text{-Si-CH}_3$ group and 1021.3 cm^{-1} and 1093–1094 cm^{-1} —characteristic for asymmetric tensile oscillation of Si–O–Si group. Based on the analysis of the FT-IR spectrums obtained, the presence of bands characteristic for symmetrical and asymmetrical deformation oscillations of Si– CH_3 groups can also be noted, with wavenumbers of 1261 cm^{-1} and 1411 cm^{-1} respectively. The bands in the range of wavenumbers 2905 cm^{-1} and 2963 cm^{-1} characteristic for tensile oscillations of C–H bonds indicate the presence of methyl groups in the silicone molecule. However, no bands in the range of 2160–2170 cm^{-1} were recorded, which indicates the absence of –SiH groups in molecules of the compounds used. There were also no differences in the occurrence of individual bands, their displacement towards higher or lower wavenumbers or significant changes in intensity of individual bands. The obtained FT-IR spectrums indicate that all silicones used are aliphatic compounds containing methyl groups, which can be classified as polydimethylsiloxanes.

3.2. Analysis of the Properties of Ceramic Elements Used to Produce Hybrid Silicone-Ceramic Composites

Ballistic properties of ceramic composites depend on several factors. These include density, porosity, hardness, tear strength, Young's modulus, acoustic impedance, mechanical strength of ceramic elements, and several other factors. A number of works [17,52–54] have shown that single properties of ceramic elements do not have a direct correlation with ballistic properties because the mechanism of tearing during a real bullet impact is very complicated. In addition, it was also determined that microstructural features affect physical and ballistic properties, causing differences in the mechanisms of tear propagation and energy dissipation and ultimately affecting ballistic properties. In order to determine which of the physico-mechanical properties are essential for the ballistic resistance of hybrid silicone ceramic composites, tests were performed to compare the properties, i.e., density, Young's modulus, hardness, acoustic impedance, and brittle fracturing resistance coefficient for two different thicknesses of ceramic elements made of alumina (Table 2), and they were correlated with the obtained for the FSP.22 fragment limit values of ballistic protection V50.

The results of the physical and mechanical tests of Al_2O_3 ceramic elements showed that there were practically no differences in the obtained values of density, fracture toughness coefficient, and acoustic impedance. In the case of the other two parameters, Young's modulus and Vickers microhardness, lower values were obtained for ceramic elements with a thickness of (3.0 ± 0.2) mm. These parameters will play a significant role in shaping the cracking mechanism during the actual impact of the projectile against the HSC composite and, consequently, affect its ballistic properties.

3.3. Fragmentation Resistance Test Results

Fragmentation resistance tests were carried out for the following groups of ballistic inserts:

- soft ballistic inserts containing 42 layers of Twaron[®]CT612;
- silicone elastomers used in conjunction with soft ballistic insert containing 42 layers of Twaron[®]CT612;
- HSC composites containing Al_2O_3 ceramics with a thickness of (3.0 ± 0.2) mm used in conjunction with soft ballistic insert containing 42 layers of Twaron[®]CT612;
- HSC composites containing Al_2O_3 ceramics with a thickness of (3.5 ± 0.2) mm used in conjunction with soft ballistic insert containing 42 layers of Twaron[®]CT612;
- HSC composites containing Al_2O_3 ceramics with a thickness of (3.5 ± 0.2) mm, without reinforcing layers in the form of Poron[®]XRDMA and Twaron[®]CT612 sheets, used in conjunction with soft ballistic insert containing 42 layers of Twaron[®]CT612.

The test results are presented in Table 5 and Figure 4.

Table 5. Fragmentation resistance test results.

No.	Sample Composition	Silicone Used in Conjunction with Soft Ballistic Armor	V50 [m/s]		
			Hybrid Silicone-Ceramic Composites (HSC) Composite Used in Conjunction with Soft Ballistic Armor, Consisting of:		Composite Used in Al_2O_3 Ceramics 3.0 mm Thickness without Reinforcing Layer
			Al_2O_3 Ceramics 3.0 mm Thickness and Reinforcing Layer	Al_2O_3 Ceramics 3.5 mm Thickness and Reinforcing Layer	
1.	MM 922	712.6 ± 20.0	1288.8 ± 20.1	1526.8 ± 21.9	1530.7 ± 24.3
2.	MM 228	709.9 ± 20.2	1324.0 ± 24.4	1538.9 ± 23.2	1554.0 ± 23.8
3.	Za 22 Mould	718.4 ± 23.2	1258.6 ± 20.6	1543.6 ± 21.8	1546.3 ± 19.8

For the soft ballistic insert, the value of the V50 ballistic protection limit was obtained equal to (619 ± 15) m/s. The use of a hybrid silicon-ceramic composite containing ceramic elements with a thickness of (3.0 ± 0.2) mm resulted in more than 2-fold increase of resistance to FSP.22 fragment. When comparing composites containing ceramic elements of different thicknesses, it can be determined that increasing the thickness of the ceramic element by about (0.5 ± 0.2) mm causes an increase in the

value of the V50 ballistic protection limit in the range of 14–18%. Changes in ballistic resistance of polyethylene composites containing ceramic elements based on SiC and Al₂O₃ ceramics, depending on the thickness of the ceramic elements used, were discussed in detail in the study of Fejdyś et al. [53]. On the basis of the results contained in this paper, it was indicated that the main parameters influencing the changes in ballistic protection values along with the change in thickness of the ceramic element are acoustic impedance and fracture toughness of ceramic elements. The acoustic impedance should be as close as possible to the acoustic impedance of the base material in the ballistic armor, and the fracture toughness (K_{1c}) should be as high as possible. The combination of these two properties gives the best ballistic armor protection when tested with 7.62 × 39 mm MSC and 5.56 × 45 mm SS 109 ammunition. In the case of tests carried out herein for silicone ceramic composites, the applied ceramics with thicknesses (3.0 ± 0.2) mm and (3.5 ± 0.2) mm show no differences in the obtained values of density, resistance to brittle fracturing and acoustic impedance. The changes of resistance to FSP.22 fragment between the developed HSC composites with different thicknesses of the ceramic element are therefore related to differences in parameters such as Young's modulus and Vickers microhardness of ceramic fittings. It can be clearly stated that with the increase of values obtained for these two parameters, the ballistic properties of the tested composite system are improved. Similar relationships resulted also from studies conducted by Kaufmann et al. [52], Krell et al. [55], or Cegła et al. [56].

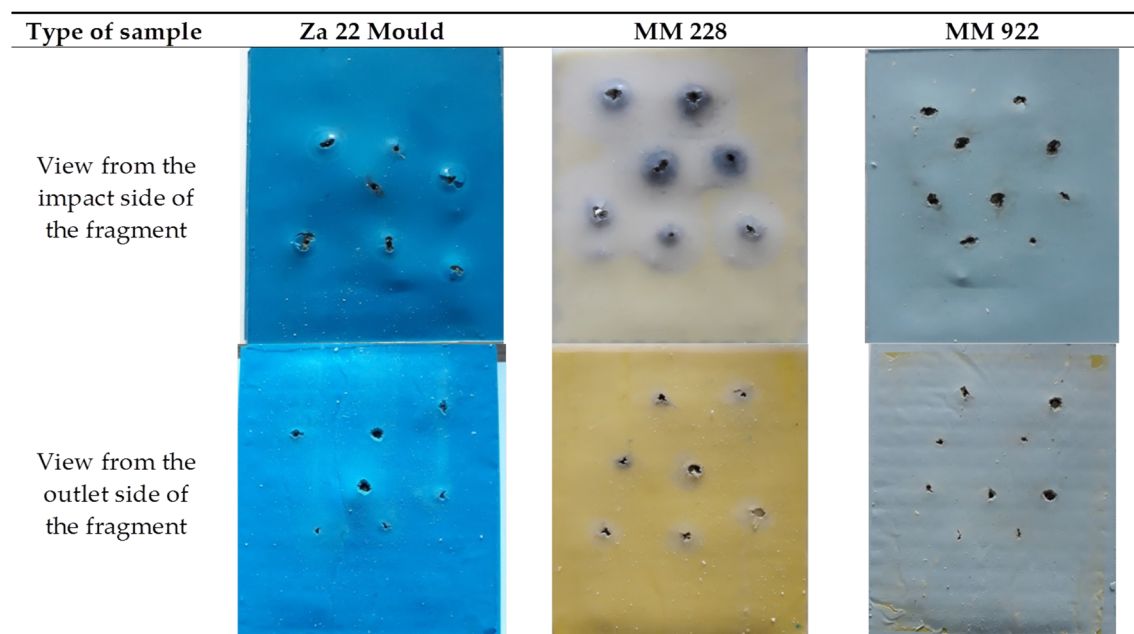


Figure 4. Hybrid ceramic-silicone composites after ballistic tests.

In addition, it was determined that there are no differences in the obtained V50 ballistic protection limit values between composites containing ceramic elements of identical thickness (3.5 ± 0.2) mm differing in the presence of reinforcement layers in the form of Poron[®]XRDMA (Polting Foam Sp. zo.o, Gliwice, Poland) and Twaron[®]CT612 (Teijin, Wuppertal, Germany) sheets. Therefore, it can be concluded that the reinforcement layers do not affect the fragmentation resistance properties of the developed composite. These layers are intended to limit the generation of secondary fragments from the ceramic fragments formed during the impact of the fragment or bullet on the sample and to contribute to the “stabilization” of the ceramic layer, understood as limiting the process of detachment of adjacent ceramic fragments under the impact of the fragment. At the same time, there is no correlation between the type of silicone elastomer used and its physical and mechanical properties (Table 1) and the obtained value of the V50 ballistic protection limit due to too minor differences between individual values of this parameter. Therefore, the lifetime as well as decomposition, viscosity, and price of the silicone elastomer for the sample preparation processes of hybrid silicone-ceramic

composites will play a role in the selection of the silicone elastomer, which may determine the speed and profitability of future production methods. On the basis of the results obtained, it can be indicated that in the case of HSC composites, the elements responsible for the absorption of impact energy at high velocities (in the range of 600–1500 m/s) are ceramics and soft ballistic inserts made of Twaron[®]CT612 (Teijin, Wuppertal, Germany). The use of silicone increases the value of the ballistic protection limit by about 100 m/s in relation to the V50 values obtained for the Twaron[®]CT612-based (Teijin, Wuppertal, Germany) soft ballistic inserts, which is about 14%.

The analysis of the literature data allowed to determine that in the case of soft ballistic inserts, four categories of factors influencing the performance and ballistic resistance of the package can be distinguished. These are: material parameters, constructional parameters, parameters of the fragment and/or bullet used for testing, and parameters of the ballistic test carried out [57,58]. The material parameters in the case of soft ballistic inserts are mainly: density of the fibers, their tensile strength, and friction occurring between the fibers. Structural parameters include: twist of the yarn, weave, thread density, number of layers, etc.

The parameters associated with the bullets, such as weight, shape, and speed, and the parameters associated with testing, such as the location of the shot, the number of shots, the angle at which the bullet hits the target, and boundary conditions can significantly affect ballistic performance. However, an in-depth discussion on bullet parameters and testing method is not the subject of this study.

In the case of material and design parameters of soft ballistic inserts, it has been observed that during an impact of a fragment or high speed bullet, its energy is absorbed by mechanisms such as yarn decrimping, fiber and yarn extension, yarn and fiberpull-out, and yarn rupture [4,59]. The relationships between the above mentioned mechanisms and the ballistic performance of the materials used for soft ballistic inserts are not yet fully described as they depend on a number of variables related to the type of materials used to produce the ballistic package and the bullet and/or fragment used. With reference to the research carried out herein, it is possible to confirm the occurrence of mechanisms, i.e., the tearing and extension of fibers and yarn of soft ballistic insert (Figure 5c,d).

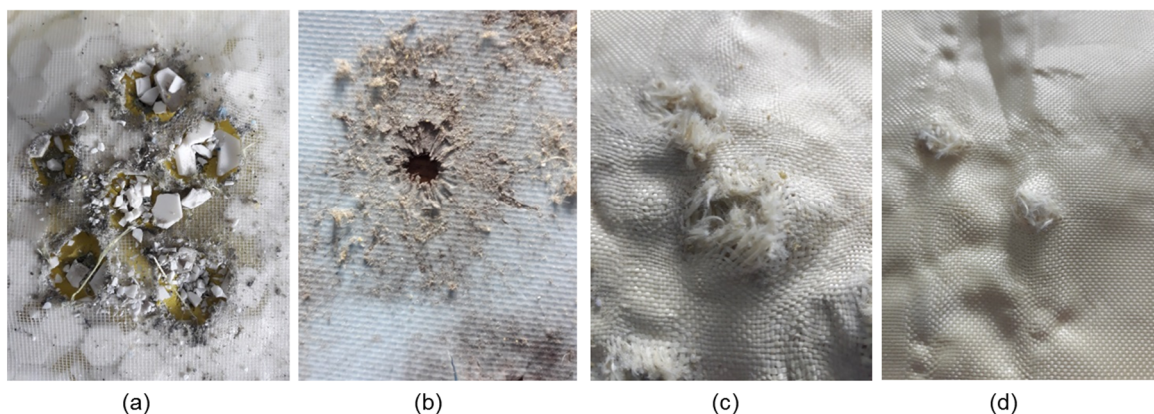


Figure 5. Components of the HSC composite after the ballistic test: (a) ceramics tiles—view from the impact side of the fragment; (b) silicone outer layer—view from the outlet side of the fragment; (c) Twaron[®]CT612 soft ballistic armor—view from the impact side of the fragment; (d) Twaron[®]CT612 soft ballistic armor—view from the outlet side of the fragment.

In turn, crushing of ceramic elements and partial delamination of the external elastomeric coating were observed for HSC composites. However, no processes related to melting or rupture of the elastomer have been reported during the fragmentation resistance tests, which is probably related to the significant thermal stability of the silicones used (Figure 5a,b).

The mechanism of rupture of ceramic elements and their influence on ballistic resistance was analyzed in previous studies. Cegła et al. [60] pointed out that the role of ceramics is to blunt the bullet's blade, break it into smaller fragments, and absorb some of its energy through fracture. He also stated

that the role of a composite made of fibrous material such as UHMWPE or para-aramid pre-impregnate, to which a ceramic layer is attached, is to stop fragments of the bullet core by elastic deformation and absorption of kinetic energy. Energy absorption takes place through combinations of deformation, fiber extension, and composite delamination [61]. When a bullet hits, the ceramic layer is exposed to very strong compressive stress. A stress wave travels through the material and when it reaches the adhesive layer, it is reflected as a tensile stress wave. The interaction of these two waves leads to cracking and destruction of the armor frontal ceramic cover. However, before this happens, the tip of the bullet is blunted or broken into smaller pieces. Therefore, it is important that the front layer of ceramics is as hard as possible [61,62]. Moreover, in the construction of the layered armor, a very important role is played by the adhesive layer between the ceramics and the fibrous substrate, which must be strong enough to ensure that after a hit, the undamaged areas of the ceramics layer and the substrate remain bound together [60].

The process of bullet penetration into the ceramic armor was also presented by Magier [63]. He described this process as a four-stage one with the individual stages:

1. bullet and armor collision;
2. initial penetration of the bullet into the armor at a constant speed;
3. braking the bullet by the inertial and strength forces of the armor material;
4. final crater formation.

In the first stage of the bullet's collision with the armor, the wave that occurs at the moment of impact propagates from the tip of the bullet to its end, generating stresses exceeding the static limit of material strength. At this stage, the tip of the bullet is plastically deformed and the shock wave moving to the end of the bullet creates a stress that causes axial cracking at its edges. As the deformation wave moves along the bullet, cracks appear. On the other hand, due to the impact, the armor creates tension and pressure, which causes the bullet's armor materials to become liquid and create a crater. At the second stage, the bullet penetrates the armor at constant speed. The crater is enlarged by the flow of the liquid phases of the bullet and armor on the sides. The back of the bullet moves faster than its tip, which then erodes. At the third stage, the high pressure field disappears and the speed of the bullet penetrating the armor is gradually lost. At the fourth stage, the crater shrinks under the influence of recrystallisation and annealing of the armor material. In addition, the mechanism of destruction of ceramic elements due to the impact of small arms ammunition was the subject of the work of Reddy et al. [64] and Hogan et al. [65].

An analogous role as presented in the above mentioned publications is played by the ceramic layer of the obtained silicon-ceramic composite. By crushing the hexagonal elements of Al_2O_3 ceramics, the fragment is blunted and some of its energy is absorbed due to the fracture of the hexagonal Al_2O_3 fittings. The outer silicone layer makes a small contribution to the fragment retention mechanism, as shown by the tests. It acts as a matrix in which the ceramic elements are placed and enables the composite system to fit the user's body, which increases the ergonomic properties of the cover.

The research also compared the value of V50 ballistic protection limit obtained for FSP.22 fragment, for HSC composites with ballistic plates manufactured from "traditional" materials, i.e., hard ballistic armor manufactured in the process of thermal-pressure pressing from Twaron[®]CT736 (Teijin, Germany), metal plates (steel and Ti-6Al-4V alloy) and ballistic hybrid plates manufactured by combining ballistic plates manufactured in the process of thermal-pressure pressing from Twaron[®]CT736 with ceramic elements or Ti-6Al-4V alloy. It should be noted that each of the above mentioned ballistic systems was placed on a soft ballistic insert made of Twaron[®]CT612 aramid with a surface mass of $(5.0 \pm 0.5) \text{ kg/m}^2$. The results are presented in Figure 6.

It has been shown that soft ballistic packets with a surface mass $(5.0 \pm 0.5) \text{ kg/m}^2$ obtained from aramid materials such as Twaron[®]CT709, CT612, or CT608 exhibit a fragmentation resistance of $(600 \pm 25) \text{ m/s}$. Retrofitting soft inserts with plates obtained from Twaron[®]CT736 aramid pre-impregnate in the process of thermo-pressure pressing increases resistance to FSP.22 fragment

from (600 ± 25) m/s to 800–1100 m/s depending on the surface mass of the tested system. Ballistic systems obtained on the basis of hybrid composites produced by combining plates obtained in the process of thermal-pressure pressing with Twaron[®]CT736 with ceramic elements or Ti-6Al-4V alloy were characterized by the highest V50 values and at the same time the highest surface mass. In this case, the resistance to FSP.22 fragment was 1580–1850 m/s. At the same time, it can be pointed out that the developed hybrid silicone-ceramic composites containing Al₂O₃ ceramic elements of thickness (3.5 ± 0.2) mm have mass per unit area comparable to a ballistic system containing steel or titanium ballistic plates at a V50 value higher by about 10%. On the basis of Figure 6, it can also be determined that the obtained HSC composites containing Al₂O₃ ceramic elements with thickness (3.0 ± 0.2) mm and mass per unit area within the limits (21.0 ± 0.5) kg/m² are characterized by higher values of ballistic protection limit V50 by about 17% in comparison to systems based on pressed Twaron[®]CT736 plates with comparable mass per unit area.

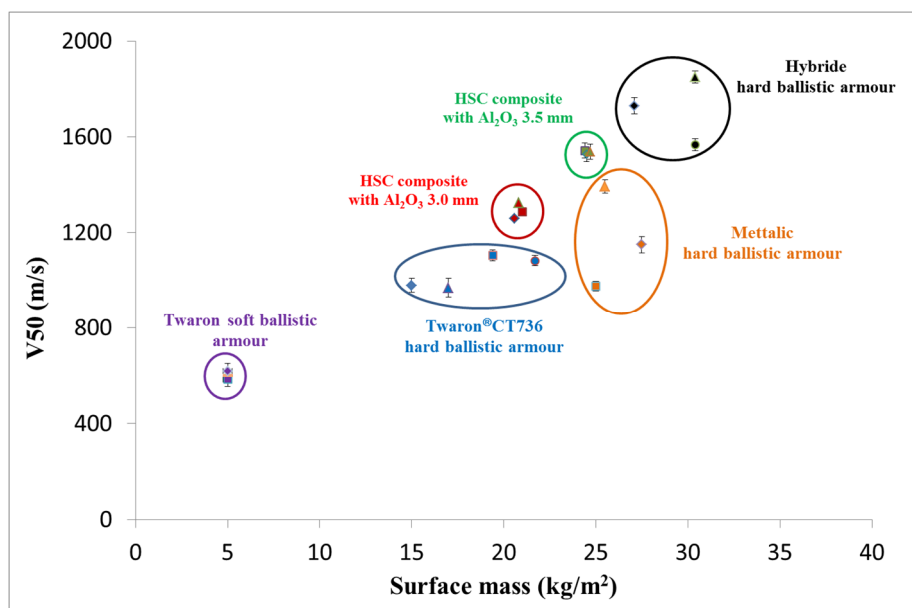


Figure 6. Dependence of V50 with the FSP.22 fragment of mass (1.10 ± 0.03) g on the surface mass for traditional ballistic systems and hybrid silicone-ceramic composites.

Thus, the conducted tests indicate that the developed hybrid silicone-ceramic composites are characterized by higher V50 parameter values for the FSP.22 fragment compared to the currently used, traditional, ballistic hard plates of comparable mass per unit area.

In addition, the obtained experimental data were also compared with the literature. For example, fragmentation tests performed by Iremonger and Went's [66] showed that laminates made using nylon 6.6 plain woven fabric and laminated with a matrix of ethylene vinyl acetate results in V50 values for 1.1 g FSPs fragment in the range of 322 to 486 m/s (depending on the number of layers of the laminate). Additionally, literature data presents polymer ceramic composites which were evaluated against fragment simulating projectiles of various calibers to investigate their ballistic impact response. Samples were prepared by mechanically mixing boron carbide (B₄C) and cubic boron nitride (cBN) over a range of ratios and combinations with either thermosetting phenolic or epoxy resin and aramid pulp. Ballistic tests performed with a 1.1 g FSP fragment for cBN-based armor results in a V50 value of approximately 784 m/s. The obtained value was almost expected as cBN is one of the hardest commercially available materials, second only to industrial diamond. Polymer ceramic composites containing B₄C tested for a V50 parameter results in a 702 m/s and Kevlar target of the same areal density results with a 680 m/s V50 parameter value [67].

The ballistic limit of the aluminum plate was investigated by the Aziz's et al. [68]. In this study, there were different types of plate arrangement. The first category was a single plate with 3 mm thickness. Meanwhile, the second category was two aluminum plates with distance of 100 mm between them. Those plates were impacted by the cylindrical FSP fragments with 6 mm long, 5 mm in diameter, and a weight of 1.1 g. The ballistic limit V50 for the single plate was equal to 276 m/s and for the double plate about 388 m/s. Much lower V50 ballistic limits were obtained for ballistic materials such as Kevlar® (DuPont, Wilmington, United States) and Twaron® aramids and Dyneema® HPPE (DSM, Heerlen, Netherlands), which were tested in a single-layer configuration. Impact velocity of carbon steel cylinder FSP fragment with 4.5 mm diameter and 0.78 g weight at 50% probability of perforation (V50) through the fabric ranged from about 120 to 250 m/s depending on the type of used material [69]. Another type of hard body armor obtained on the basis of poly (methyl methacrylate) (PMMA) and polycarbonate (PC) laminates was investigated by Hsieh and co-workers [70]. The ballistic measurements were carried out using the 1.1 g weight 0.22 caliber FSP fragments. Authors showed that the PC-PMMA-PC laminates exhibit a 37% higher value of the V50 (846 m/s) when compared with the PC-PC-PC laminates of equivalent overall layer configuration. The ballistic limit against the FSP.22 increased with increasing plate thickness of PMMA.

Comparing the literature data with results obtained for the developed HSC composites concludes that these composites provide higher ballistic protection than various types of laminates, aluminum plates, or polymer ceramic composites with B₄C or cBN ceramics.

3.4. Impact Test Results

The obtained silicon-ceramic composites were also subjected to impact forces generated at much lower velocities (about 1–10 m/s) during falls that occurred during various types of physical activities (roller sports, cycling, horse riding). The obtained results are summarized and presented in Figure 7 and Table 6.

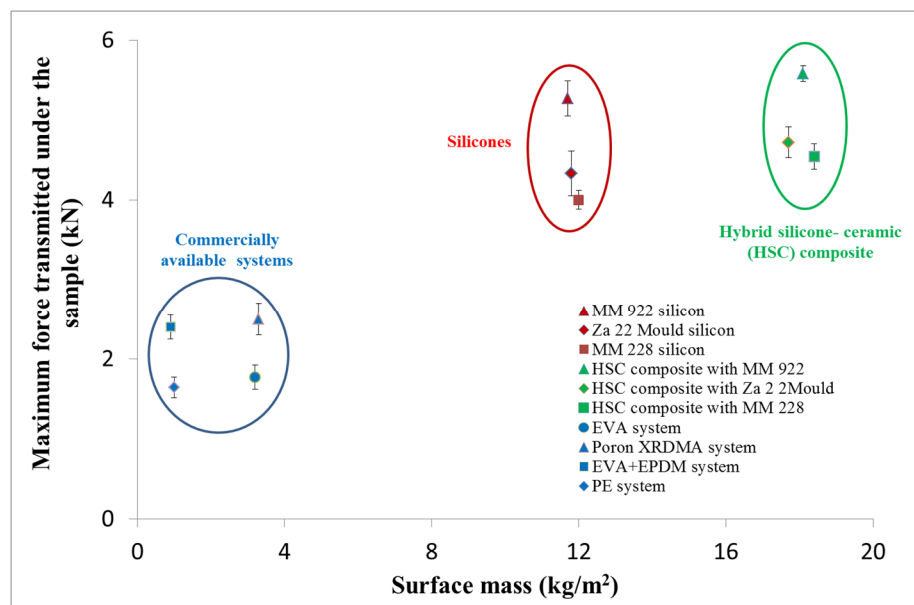


Figure 7. Dependence of the maximum force transferred to the sample on the surface mass of the tested composite systems.

Slightly higher values of the maximum force transmitted under the sample were obtained for hybrid silicone-ceramic composites compared to samples consisting only of silicone elastomers of the same thickness. It should be noted that HSC composites show a much higher mass per unit area (increase by about 50%) compared to samples based only on silicone elastomers (Table 6). In view of

the above, it can be clearly indicated that the presence of ceramic elements does not improve the shock absorption capacity during impact with 5 J affecting the composite. However, in the case of impact tests, it is possible to indicate the relationship between the type of silicone elastomer used and the maximum value of energy transferred to the sample. The lowest values for both the composite and the elastomer sample were obtained for MM 228 silicone, whereas the highest for MM 922. Analyzing the obtained test results in terms of correlation between the ability to absorb impact energy and the physical and mechanical parameters, it can be indicated that only in the case of tear strength, the following relation was noted, i.e., the increase in tear strength was accompanied by a decrease in the value of maximum force transmitted to the sample. For the remaining parameters, i.e., hardness, density, extension at tear, and tensile strength, no dependence on the ability to absorb impact energy was determined.

Table 6. Impact test results for the impact energy of 5 J.

No.	Composition of Samples	Surface Mass (kg/m ²)	Maximum Force Transmitted under the Sample (kN)
Silicone samples:			
1.	MM 922 silicon	11.7 ± 0.4	5.27 ± 0.22
2.	MM 228 silicon	12.0 ± 0.5	4.00 ± 0.12
3.	Za 22 Mould silicon	11.8 ± 0.5	4.33 ± 0.28
Hybrid silicone-ceramic composite containing Al ₂ O ₃ ceramics (3.0 mm thick) and silicone:			
4.	MM 922	18.1 ± 0.5	5.58 ± 0.10
5.	MM 228	18.4 ± 0.6	4.54 ± 0.16
6.	Za 22 Mould	17.7 ± 0.6	4.72 ± 0.19
Samples of commercial systems containing polymer:			
7.	EVA	3.2 ± 0.3	1.77 ± 0.17
8.	Poron®XRDMA	3.3 ± 0.3	<4.0
9.	EVA+EPDM	0.9 ± 0.2	2.40 ± 0.15
10.	PE	1.0 ± 0.4	1.64 ± 0.13

The results obtained for silicone samples and HSC composites were also compared with commercially available materials such as Poron®XRDMA, EVA copolymer, polyethylene, used in market products intended for the production of protectors reducing the risk of human body injury. The tests were performed for an impact energy of 5 J, for samples with thicknesses corresponding to the remaining composite samples (Table 6). In this case, it has been determined that both the silicone elastomers and hybrid silicone ceramic composites used have a poorer ability to absorb impact energy with a significantly higher mass per unit area, which excludes them from use on an industrial scale in the construction of protectors. However, the obtained results did not allow to indicate the reasons for poor ability to absorb impact energy generated at low speeds of 1–10 m/s for the developed composites, as they depend on many factors, such as: properties of the composite used, its physical-mechanical parameters, shape and geometry of the sample or the value of the applied load, as well as on the processes occurring during impact, i.e., deformations, plastic and/or elastic deformations, cracks, delamination, thermal effects, and others. This may be a challenge for further research work.

4. Conclusions

As a part of the work, hybrid silicone-ceramic composites were obtained. These composites in combination with a soft ballistic armor with an area weight (5.0 ± 0.5) kg/m² provide V50 ballistic protection limit in the range of 1200–1500 m/s. The developed HSC composite may be an alternative to the currently used ballistic composites produced in the thermal-pressure pressing process based on aramid or UHMWPE materials, as well as steel or titanium alloy ballistic armor. The research showed that the ballistic resistance of the HSC composite is the result of the destruction of ceramic elements by the fragment and the pulling, rupture, decrimbing, and extension of yarns and fibers occurring in the soft ballistic insert. It was determined that the V50 value increases as the thickness of

the ceramic element increases. An increase in the thickness of the Al_2O_3 ceramic element by about (0.5 ± 0.2) mm resulted in an increase in the V50 value in the range of 14–18%. The decisive factors here were the physical and mechanical parameters of ceramic elements, i.e., hardness and Young's modulus. The outer silicone layer makes a slight contribution to the fragments' stopping mechanism, as demonstrated in the research. It acts as a matrix in which ceramic elements are placed and allows the composite system to adjust to the user's body, which increases the ergonomic properties of the armor. The conducted research allowed to determine that there are no correlations between the type of silicone elastomer used and its physico-mechanical properties, and the obtained value of the V50 ballistic protection limit.

Comparison of the results for the impact energy equal to 5 J generated during the drop tower tests, obtained for samples of HSC composites with commercially available materials used in market products intended for the production of protectors reducing the risk of human body damage, indicated that the hybrid silicone-ceramic composites had lower ability to shock absorption with a significantly higher surface weight. Therefore, they should be excluded from use on an industrial scale in the construction of these type of protectors.

Designing of energy absorbing materials is challenging since various mechanisms, such as: wave propagation, dynamic cracks, delamination, thermal effects, dislocation generation, elastic and shear deformations, yarn and fiber pull-out and rupture, etc. are acting concurrently, at different material scales, and intertwined during impact. Therefore, new research is needed, especially in producing materials with strictly defined characteristics, modeling, and simulation of impact to be able to reach a point where the designed composites will meet all user's requirements related to low weight, ergonomics, and ballistic resistance.

5. Patents

The work reported in this manuscript based on the Patent no. PL 424443(A1)—Method for producing flexible ballistic armor and the armor produced by this method.

Author Contributions: Conceptualization, K.K. and K.O.; methodology, K.K., M.L., and E.C.-F.; formal analysis, K.K., M.L.; investigation, K.K., M.L., P.K., and E.C.-F.; resources, K.K. and P.K.; writing—original draft preparation, K.K.; visualization, K.K.; writing—review, M.F.; supervision, M.F. and K.K.; project administration, M.F. All authors have read and agreed to the published version of the manuscript.

Funding: This research was funded by the National Centre for Research and Development, Research Grant No. POIR.04.01.04-00-0007/18-00 implemented as part of the Smart Growth Operational Programme 2014–2020.

Conflicts of Interest: The authors declare no conflict of interest.

References

1. Kumar, N. Bulletproof vest and its improvement—A review. *IJTSRD* **2016**, *1*, 34–39.
2. Yang, Y.; Chen, X. Determination of materials for hybrid design of 3D soft body armour panels. *Appl. Compos. Mater.* **2018**, *25*, 861–875. [[CrossRef](#)]
3. Yang, Y.; Chen, X. Investigation on energy absorption efficiency of each layer in ballistic armour panel for applications in hybrid design. *Compos. Struct.* **2017**, *164*, 1–9.
4. Mawkhlieng, U.; Majumdar, A.; Laha, A. A review of fibrous materials for soft body armour applications. *RSC Adv.* **2020**, *10*, 1066–1086. [[CrossRef](#)]
5. National Institute for Justice. *0101.04 Standard, Ballistic Resistance of Personal Body Armour*; U.S. Department for Justice: Washington, DC, USA, 2000.
6. Azrin Hani, A.R.; Roslan, A.; Mariatti, J.; Maziah, M. Body armor technology: A review of materials, construction techniques and enhancement of ballistic energy absorption. *Adv. Mat. Res.* **2012**, *488–489*, 806–812.
7. Perry, A. Ballistic-resistant body armor: Problems and coping strategies. *J. Text. Appar. Technol. Manag.* **2018**, *10*, 1–14.

8. Fejdyś, M.; Kośła, K.; Kucharska-Jastrzabek, A.; Landwijt, M. Hybride composite armour systems with advanced ceramics and ultra-high molecular weight polyethylene (UHMWPE) fibres. *Fibres Text. East. Eur.* **2016**, *24*, 79–89. [CrossRef]
9. Crouch, I.G. Body armour—New materials, new systems. *Def. Technol.* **2019**, *15*, 241–253. [CrossRef]
10. Cegła, M.; Habaj, W.; Stepniak, W.; Podgórzak, P. Hybrid ceramic-textile composite armour structures for a strengthened bullet-proof vest. *Fibres Text. East. Eur.* **2015**, *23*, 85–88.
11. Ruys, A.J. (Ed.) Alumina in lightweight body armor. In *Alumina Ceramics: Biomedical and Clinical Applications*; Woodhead Publishing: Cambridge, UK, 2019; pp. 321–368.
12. Bracamonte, L.; Loutfy, R.; Yilmazcoban, I.K.; Rajan, S.D. Design, manufacture, and analysis of ceramic-composite armor. In *Lightweight Ballistic Composites: Military and Law-Enforcement Applications*, 2nd ed.; Bathnagar, A., Ed.; Woodhead Publishing: Cambridge, UK, 2016; pp. 349–367.
13. Su, C.; Chen, B. Study on effective protective area of ceramic composite target. *IOP Conf. Ser. Mater. Sci. Eng.* **2020**, *768*, 1–7. [CrossRef]
14. Song, H.; Bless, S.J.; Jang, S.-D. Tile size dependency of ballistic performance in alumina. *J. Korean Ceram. Soc.* **1995**, *32*, 366–370.
15. Hazell, P.J.; Roberson, C.J.; Moutinho, M. The design of mosaic armour: The influence of tile size on ballistic performance. *Mater. Des.* **2008**, *29*, 1497–1503. [CrossRef]
16. Appleby-Thomas, G.J.; Jaansalu, K.; Hameed, A.; Painter, J.; Shackel, J.; Rowley, J. A comparison of the ballistic behaviour of conventionally sintered and additively manufactured alumina. *Def. Technol.* **2020**, *16*, 275–282. [CrossRef]
17. Medvedovski, E. Ballistic performance of armour ceramics: Influence of design and structure. Part 1. *Ceram. Int.* **2010**, *36*, 2103–2115.
18. Okhawilai, M.; Hiziroglu, S.; Rimdusit, S. Measurement of ballistic impact performance of fiber reinforced polybenzoxazine/polyurethane composites. *Measurement* **2018**, *130*, 198–210. [CrossRef]
19. Camoso Pereira, A.; Salgado de Assis, F.; Costa Garcia Filho, F.; Souza Oliveira, M.; Cruz Demosthenes, L.C.; Colorado Lopera, H.A.; Neves Monteiro, S. Ballistic performance of multilayered armor with intermediate polyester composite reinforced with fique natural fabric and fibers. *J. Mater. Res. Technol.* **2019**, *8*, 4221–4226. [CrossRef]
20. Costa Garcia Filho, F.C.; Monteiro Neves, S. Piassava fiber as an epoxy matrix composite reinforcement for ballistic armor applications. *JOM* **2019**, *71*, 801–808.
21. Abdullah, S.; Abdullah, M.F.; Jamil, W.N.M. Ballistic performance of the steel-aluminium metal laminate panel for armoured vehicle. *J. Mech. Eng. Sci.* **2020**, *14*, 6452–6460. [CrossRef]
22. Kędzierski, P.; Gieleta, R.; Morka, A.; Niezgodna, T.; Surma, Z. Experimental study of hybrid soft ballistic structures. *Compos. Struct.* **2016**, *153*, 204–211. [CrossRef]
23. Goode, T.; Shoemaker, G.; Schultz, S.; Peters, K.; Pankow, M. Soft body armor time-dependent back face deformation (BFD) with ballistics gel backing. *Compos. Struct.* **2019**, *220*, 687–698. [CrossRef]
24. Varma, T.V.; Sarkat, S. Designing polymer metamaterial for protective armor: A coarse-grained formulation. *Meccanica* **2020**, 1–10. [CrossRef]
25. Colombo, P.; Zordan, F.; Medvedovski, E. Ceramic-polymer composites for ballistic protection. *Adv. Appl. Ceram.* **2006**, *105*, 78–83. [CrossRef]
26. Cohen, M. Composite Armor Plate. U.S. Patent 2,005,007,229,4A1, 7 April 2005.
27. Wiśniewski, A.B.; Pacek, D.B.; Żochowski, P.; Wierzbicki, Ł.; Kozłowska, J.; Zielińska, D.; Olszewska, K.; Grabowska, G.; Błaszczak, J.; Pawłowska, A.; et al. Elastic Armour. Patent No. PL224825 (B1), 28 February 2017.
28. Gamache, R.M.; Roland, C.M. Body Armor of Ceramic Ball Embedded Polymer. U.S. Patent 2,012,031,215,0A1, 13 December 2012.
29. Martin, C.A.; Lee, G.F.; Fedderly, J.J. Composite Ballistic Armor Having Geometric Ceramic Elements for Shock Wave Attenuation. U.S. Patent 768,592,2B1, 30 March 2010.
30. National Institute for Justice. *Standard 0117.01 Public Safety Bomb Suit Standard*; U.S. Department for Justice: Washington, DC, USA, 2016.
31. PBCH-09/2017. Density Determination by Hydrostatic Method.
32. PN-EN ISO 868:2005. Plastics and Ebonite—Determination of Identification Hardness by Means of Durometer (Shore Hardness). Available online: <https://sklep.pkn.pl/pn-en-iso-868-2005p.html> (accessed on 19 December 2020).

33. PN-ISO-37:2007 Rubber, Vulcanized or Thermoplastic—Determination of Tensile Stress-Strain Properties. Available online: <https://sklep.pkn.pl/pn-iso-37-2007p.html> (accessed on 19 December 2020).
34. BS EN 993-1:1995, Methods of Test for Dense Shaped Refractory Products—Part 1: Determination of Bulk Density, Apparent Porosity and True Porosity. Available online: https://infostore.saiglobal.com/en-us/standards/bs-en-993-1-1995-204239_saig_bsi_bsi_484986/ (accessed on 19 December 2020).
35. ASTM C 1419-99a, Standard Test Method for Sonic Velocity in Refractory Materials at Room Temperature and Its Use in Obtaining an Approximate Young's Modulus. Available online: <https://www.astm.org/DATABASE.CART/HISTORICAL/C1419-99A.htm> (accessed on 19 December 2020).
36. PN-EN ISO 6507-1:2018-05, Metallic Materials—Vickers Hardness Test—Part 1: Test Method. Available online: <https://sklep.pkn.pl/pn-en-iso-6507-1-2018-05p.html> (accessed on 19 December 2020).
37. PN-EN 1773:2003 Textiles—Flat Textiles—Determination of Width and Length. Available online: <https://sklep.pkn.pl/pn-en-1773-2000p.html> (accessed on 19 December 2020).
38. PN-ISO 3801:1993 Textiles—Fabrics—Determination of Linear and Area Mass. Available online: <https://sklep.pkn.pl/pn-iso-3801-1993p.html> (accessed on 19 December 2020).
39. PN-EN 1049-2:2000 Textiles—Methods for Analyzing the Structure of Woven Products—Determining the Number of Threads Per Unit Length. Available online: https://infostore.saiglobal.com/en-us/standards/PN-EN-1049-2-2000-932508_SAIG_PKN_PKN_2198013/ (accessed on 19 December 2020).
40. PN-EN ISO 5084:1999 Textiles—Determination of Thickness of Textiles and Textile Products. Available online: <https://www.iso.org/standard/23348.html> (accessed on 19 December 2020).
41. PN-EN ISO 13934-1:2013-07 Textiles—Tensile Properties of Fabrics—Part 1: Determination of Maximum Force and Elongation at Maximum Force Using the Strip Method. Available online: <https://sklep.pkn.pl/pn-en-iso-13934-1-2013-07e.html> (accessed on 19 December 2020).
42. PN-EN ISO 2286-2:2016-11 Rubber- or Plastics-Coated Fabrics. Determination of Roll Characteristics. Methods for Determination of Total Mass Per Unit Area, Mass Per Unit Area of Coating and Mass Per Unit Area of Substrate. Available online: <https://sklep.pkn.pl/pn-en-iso-2286-2-2016-11e.html> (accessed on 19 December 2020).
43. PN-EN ISO 1798:2001 Flexible Cellular Polymeric Materials—Determination of Tensile Strength and Elongation at break. Available online: <https://sklep.pkn.pl/pn-en-iso-1798-2001p.html> (accessed on 19 December 2020).
44. PN-EN ISO 8067:2009 Flexible Cellular Polymeric Materials Tear Strength. Available online: <https://standards.iteh.ai/catalog/standards/sist/a014d72d-6be9-401e-914f-c2a35767afc7/sist-en-iso-8067-2009> (accessed on 19 December 2020).
45. PBCH-02/2014 Spectrophotometric Analysis of Spectra in the Aspect of Determining the Raw Material Composition in Selected Textile Materials.
46. PN-79/H-04361, Measuring the Hardness of Metals Vickers Method With Loads of Less Than 9.8 N.
47. PN-EN ISO 4674-1:2017-02 Rubber—Or Plastics-Coated Fabrics—Determination of Tear Resistance—Part 1: Constant Rate of Tear Methods. Available online: https://sklep.pkn.pl/catalogsearch/advanced/result/?date_publication%5Bfrom%5D=oybrdlui&dir=desc&limit=25&order=standard_number&p=1585 (accessed on 19 December 2020).
48. PBB-09 Ballistic research. Determination of Fragment Resistance of a Set of Samples.
49. STANAG 2920 Ballistic Test Method for Personal Armour Materials and Combat Clothing.
50. PBB-07 ed. II: 12.2008 Impact tests. Determining the level of impact energy attenuation for body protectors.
51. BS 7971-1:2002 Protective Clothing and Equipment for Use in Violent Situations and in Training. General Requirements. Available online: <https://shop.bsigroup.com/ProductDetail/?pid=00000000030016991> (accessed on 19 December 2020).
52. Kaufmann, C.; Cronin, D.; Worswick, M.; Pageauband, G.; Beth, A. Influence of material properties on the ballistic performance of ceramics for personalbodyarmour. *Shock. Vib.* **2003**, *10*, 51–58. [[CrossRef](#)]
53. Fejdyś, M.; Kośla, K.; Kucharska-Jastrzabek, A.; Łandwjit, M. Influence of ceramic properties on the ballistic performance of the hybrid ceramic—Multi-layered UHMWPE composite armour. *J. Aust. Ceram. Soc.* **2020**, *56*, 1–13. [[CrossRef](#)]
54. Rahbek, D.B.; Johnsen, B.B. *Dynamic Behaviour of Ceramic Armour Systems*; Report of the Norwegian Defence Research Establishment (FFI): Kjeller, Norway, 2015; ISBN 978-82-464-2609-9.

55. Krell, A.; Strassburger, E. Order of influences on the ballistic resistance of armor ceramics and single crystals. *Mater. Sci. Eng.* **2014**, *597*, 422–430. [[CrossRef](#)]
56. Cegła, M.; Habaj, W.; Podgórzak, P. Carbide ceramics in lightweight armour applications. *Cer. Mater.* **2015**, *2*, 132–136.
57. Arora, S.; Ghosh, A. Evolution of soft body. In *Advanced Textile Engineering Materials*; ul-Islam, S., Butola, B.S., Eds.; Wiley Scrivener: Austin, TX, USA, 2018; pp. 499–552.
58. Naik, N.K.; Shrirao, P. Composite structures under ballistic impact. *Compos. Struct.* **2004**, *66*, 579–590. [[CrossRef](#)]
59. Majumdar, A.; Butola, B.S.; Srivastava, A. An analysis of deformation and energy absorption modes of shear thickening fluid treated Kevlar fabrics as soft body armour materials. *Mater. Des.* **2013**, *51*, 148–153. [[CrossRef](#)]
60. Cegła, M. Special ceramics in multilayer ballistic protection systems. *Issues Armament Technol.* **2018**, *147*, 63–74. [[CrossRef](#)]
61. Grujicic, M.; Pandurangan, B.; Zecevic, U.; Koudela, K.L.; Cheeseman, B.A. Ballistic Performance of Alumina/S-2 glass reinforced polymer-matrix composite hybrid lightweight armor against armor piercing (AP) and non-AP projectiles. *Multidiscip. Model. Mater. Struct.* **2007**, *3*, 287–312. [[CrossRef](#)]
62. Demir, T.; Ubeyli, M.; Yildirim, R.; Karakas, M.S. Investigation on the ballistic performance of alumina/4340 steel laminated composite armor against 7.62 mm armor piercing projectiles. *Metal* **2008**, *3*, 1–7.
63. Magier, M. Methods of estimating the armor penetration depth by kinetic projectiles. *Issues Armament Technol.* **2007**, *101*, 103–115.
64. Rama Subba Reddy, P.; GeasinSavio, S.; Madhu, V. Ceramic composite armour for ballistic protection. In *Handbook of Advanced Ceramics and Composites*; Mahajan, Y., Roy, J., Eds.; Springer: Cham, Switzerland, 2019; pp. 1–43.
65. Hogan, J.D.; Farbaniec, L.; Mallick, D.; Domnich, V.; Kuwelkar, K.; Sano, T.; McCauley, J.W.; Ramesh, K.T. Fragmentation of an advanced ceramic under ballistic impact: Mechanisms and microstructure. *Int. J. Impact Eng.* **2017**, *102*, 47–54. [[CrossRef](#)]
66. Iremonger, M.J.; Went, A.C. Ballistic impact of fibre composite armours by fragment-simulating projectiles. *Compos. Part A Appl. Sci. Manuf.* **1996**, *27A*, 575–581. [[CrossRef](#)]
67. Naebe, M.; Sandlin, J.; Crouch, I.; Fox, B. Novel polymer-ceramic composites for protection against ballistic fragments. *Polym. Compos.* **2013**, *34*, 180–186. [[CrossRef](#)]
68. Aziz, M.R.; Zainol, M.F.; Othman, R. An experimental study on ballistic limit of aluminum plate subjected to fragment-simulating projectile. *J. Fail. Anal. Preven.* **2020**, *20*, 2059–2064. [[CrossRef](#)]
69. Nguyen, T.-T.N.; Meek, G.; Breeze, J.; Masouros, S.D. Gelatine Backing affects the performance of single-layer ballistic-resistant materials against blast fragments. *Front. Bioeng. Biotechnol.* **2020**, *8*, 1–10. [[CrossRef](#)]
70. Hsieh, A.J.; DeSchepper, D.; Moy, P.; Dehmer, P.G.; Song, J.W. *The Effects of PMMA on Ballistic Impact Performance of Hybrid Hard/Ductile All-Plastic- and Glass-Plastic-Based Composites*; Army Research Laboratory, Aberdeen Proving Ground, MD: Aberdeen, WA, USA, 2004.

Publisher's Note: MDPI stays neutral with regard to jurisdictional claims in published maps and institutional affiliations.



© 2020 by the authors. Licensee MDPI, Basel, Switzerland. This article is an open access article distributed under the terms and conditions of the Creative Commons Attribution (CC BY) license (<http://creativecommons.org/licenses/by/4.0/>).